Electronic Research Archive

http://www.aimspress.com/journal/era

ERA, 33(1): 26–49.
DOI: 10.3934/era.2025002
Received: 09 October 2024
Revised: 23 November 2024
Accepted: 10 December 2024
Published: 06 January 2025

Research article

Complex dynamics of non-smooth pest-natural enemy Gomportz models with a variable searching rate based on threshold control

Yuan Tian[1,*], Xinlu Tian[1], Xinrui Yan[1], Jie Zheng[2] and Kaibiao Sun[3,*]

[1] School of Science, Dalian Maritime University, Dalian 116026, China
[2] Liaoning Ocean and Fisheries Science Research Institute, Dalian 116023, China
[3] School of Control Science and Engineering, Dalian University of Technology, Dalian 116024, China

* **Correspondence:** Email: tianyuan@dlmu.edu.cn, sunkb@dlut.edu.cn.

Abstract: The implementation of ecological pest-management strategies is an important trend in the global agricultural development, which makes integrated pest management become an important research field. In this study, to achieve a scientific and reasonable pest-management objective, three aspects of work were carried out. 1) *Modeling and analysis*: a pest-natural enemy Gomportz-type model with a variable searching rate was put forward, and two pest-management models were formulated. The dynamic characteristics of the continuous model were investigated, and the results indicated that the search speed of natural enemies had an effect on the coexistence equilibrium. 2) *Control effect*: the sliding mode dynamics of the Filippov system including the existence of pseudo-equilibrium was analyzed to illustrate the effect of the non-smooth control strategy on the system. A Poincaré map was constructed for the system with a threshold control, and the complex dynamics induced by the threshold control was investigated. 3) *Verifications*: computer simulations were presented step by step to illustrate and verify the correctness of the theoretical results. A comprehensive study of predation relationships as well as the effects of different management strategies on the system can serve as a valuable reference for advancing sustainable agricultural practices and pest control.

Keywords: Filippov system; order-k periodic trajectory; Poincaré map; orbital asymptotic stability

1. Background and motivation

One of the most significant trends in global agricultural development is the ecological management of pests. From the perspective of ecosystem integrity, reducing and controlling pests through biological and ecological control are of great significance for the construction of ecological civilization. Biological and ecological control can reduce management cost, maintain ecological

stability, and avoid environmental pollution and damage to biodiversity. As a large agricultural country, China places a premium on green prevention and control within its agricultural sector and proposed the National Strategic Plan for Quality Agriculture (2018–2022), which proposes to implement green prevention and control actions instead of chemical control and achieve a coverage rate of more than 50% for green prevention and control of major crop pests. The Crop Pests Regulations on the Prevention and Control of Crop Pests prioritizes the endorsement and support of green prevention and control technologies such as ecological management, fosters the widespread application of information technology and biotechnology, and propels the advancement of intelligent, specialized, and green prevention and control efforts [1]. Therefore, the simulation of pest dynamic behavior and the research of control strategies are helpful for more scientific and reasonable pest management.

In a natural ecosystem, the predator-prey relationship is one of the most important relationships, and has become a main topic in ecological research and widely studied by scholars in recent years. Depending on the problem under consideration and the biological background, related research can be divided into two forms: ordinary differential [2–5] and partial differential [6–11]. The earliest work on the mathematical modeling of predation relationships dates back to the twentieth century, named as the Lotka-Volterra model [12, 13]. Subsequently, scholars have extended the Lotka-Volterra model in different directions such as introducing different types of growth functions [14–16] and different forms of functional response [17–20]. The Gompertz model [14] is one of the most frequently used sigmoid models fitted to growth data and other. Scholars have fitted the Gompertz model to everything from plant growth, bird growth, fish growth, and growth of other animals [21–23]. Compared with the logistic model, it is more suitable for pest or disease curve fitting with S-shaped curve asymmetry, and fast development at first and slow development later. In addition, the Holling-II functional response function is the most commonly employed one, in which the searching rate is considered as a constant. Nevertheless, in the real world, the density of the prey and the predator's searching environment can affect the predator's searching speed. Consequently, Hassell et al. [24] proposed a saturated searching rate. Guo et al. [25] introduced a fishery model with the Smith growth rate and the Holling-II functional response with a variable searching rate. In this work, a pest-natural enemy model with the Gomportz growth rate and a variable searching rate is investigated.

To prevent the spread of pests, effective control action should be implemented before the pests cause a certain amount of damage to the environment and crops. One way is to slow down the spreading speed of pests by setting a warning threshold, and when the density of pests exceeds this threshold level, an integrated control measure is imposed on the system. This kind of control system can be modeled by a Filippov system, which has been recognized by scholars and widely used in the study of concrete models with one threshold [26–31], a ratio-dependent threshold [32], or two thresholds [33]. In this study, we will also focus on Filippov predation models with dual thresholds. In addition, considering the instantaneous behavior of the control, an integrated pest-management strategy with threshold control is adopted, which is an instantaneous intervention imposed on the system and always taken as a practical approach for pest management. In recent years, there has been a lot of research and application of impulsive differential equations (IDEs) in population dynamics to model the instantaneous intervention activities. There are mainly six types of models involved in the research: periodic [34–37], prey-dependent [38–43], predator-dependent [44], ratio-dependent [45], nonlinear prey-dependent [46], and combined prey-predator dependent [47–51]. In the context of

integrated pest management, setting a threshold for pest population density to control its spread is crucial. Therefore, in this study, we introduce a pest economic threshold: when the pest population density exceeds this threshold, we will intervene manually, which includes not only spraying pesticides but also releasing natural enemies.

The article is organized in the following way: In Section 2, an integrated pest-management model with a variable searching rate based on double-threshold control is proposed. In Section 3, a dynamical analysis of the continuous system is performed, including the positivity and boundedness of the solutions, the existence and local stability of equilibrium points, and the dynamic behavior of the Filippov pest-management model with double thresholds. In Section 4, the complex dynamic behavior of the system induced by the economic threshold feedback control is focused on. In Section 5, numerical simulations are carried out to illustrate the main results of the above two sections step by step and to illustrate the practical implications. Finally, a summary of the research work is presented, and future research directions are discussed.

2. Model formulation and preliminaries

2.1. Pest control model

A pest-natural enemy Gomportz model with a variable searching rate and Holling-II functional response is considered:

$$\begin{cases} \dfrac{\mathrm{d}x}{\mathrm{d}t} = rx(\ln K - \ln x) - b(x)\dfrac{xy}{1+hx}, \\ \dfrac{\mathrm{d}y}{\mathrm{d}t} = b(x)\dfrac{exy}{1+hx} - dy, \end{cases} \tag{2.1}$$

where x (y) represents the pest's (natural enemies) density, respectively; r represents the pest's intrinsic growth rate; K represents the pest's environmental carrying capacity; $b(x) = bx/(x+g)$ represents the variable searching rate [24, 25] with maximum searching rate b and saturated constant g; e represents the conversion efficiency; and d represents the predator's natural mortality. All parameters are positive, and b, e and d are less than one. In addition, it requires that $eb - dh > 0$, i.e., the natural enemy species can survive when pests are abundant.

To prevent the rapid spread of pests, two control methods are adapted: one is the continuous control with two thresholds, that is, when the pest density is below the pest warning threshold x_{ET}, no control measures need to be taken, when the pest and natural enemy densities satisfy $x > x_{ET}$ and $y < y_{ET}$, the control action by spraying pesticides and releasing a part (q_1) of the natural enemies is taken, which causes the death of pests (p_1) and natural enemies (q_2), when their densities satisfy $x > x_{ET}, y > y_{ET}$, only spraying pesticides is adapted. Based on the above control strategy, the impulsive control system can be formulated as follows:

$$\begin{cases} \dfrac{\mathrm{d}x}{\mathrm{d}t} = rx(\ln K - \ln x) - \dfrac{bx^2y}{(1+hx)(x+g)} - \delta_1(x,y)x, \\ \dfrac{\mathrm{d}y}{\mathrm{d}t} = \dfrac{ebx^2y}{(1+hx)(x+g)} - dy + \delta_2(x,y)y, \end{cases} \tag{2.2}$$

where

$$(\delta_1(x,y),\delta_2(x,y)) = \begin{cases} (0,0), x < x_{ET}, \\ (p_1, q_1 - q_2), x > x_{ET}, y < y_{ET}, \\ (p_1, -q_2), x > x_{ET}, y > y_{ET}. \end{cases} \tag{2.3}$$

Another one is an intermittent control with an economic threshold, that is, when the pest's density is below an economic threshold, no control action is implemented. Once the pest's density reaches the economic threshold, the control action by spraying pesticides and releasing a nonlinear volume $\frac{\tau}{1+ly}$ of natural enemies is taken, which causes the death of pests (p_1) and natural enemies (q_2), where τ and $l > 0$ are the formal parameters of the maximum volume of predators, respectively. Based on this control strategy, we can formulate the impulsive control system as follows:

$$\begin{cases} \left.\begin{aligned} \frac{\mathrm{d}x}{\mathrm{d}t} &= rx(\ln K - \ln x) - \frac{bx^2y}{(1+hx)(x+g)} \\ \frac{\mathrm{d}y}{\mathrm{d}t} &= \frac{ebx^2y}{(1+hx)(x+g)} - dy \end{aligned}\right\} x < x_{ET}, \\ \left.\begin{aligned} x(t^+) &= (1-p_1)x(t) \\ y(t^+) &= (1-q_2)y(t) + \frac{\tau}{1+ly(t)} \end{aligned}\right\} x = x_{ET}. \end{cases} \tag{2.4}$$

The aim of this study focuses on analyzing the effects of different control measures on the dynamics of Models (2.2) and (2.4), respectively.

2.2. Basic knowledge

2.2.1. Filippov system

Consider a piecewise-continuous system

$$\begin{pmatrix} \frac{\mathrm{d}x}{\mathrm{d}t} \\ \frac{\mathrm{d}y}{\mathrm{d}t} \end{pmatrix} = \begin{cases} \mathbf{F}_1(x,y) & \text{if } (x,y) \in \mathrm{S}_1, \\ \mathbf{F}_2(x,y) & \text{if } (x,y) \in \mathrm{S}_2, \end{cases} \tag{2.5}$$

where

$$\mathrm{S}_1 = \{(x,y) \in \mathbb{R}^+ : H(x,y) > 0\}, \mathrm{S}_2 = \{(x,y) \in \mathbb{R}^+ : H(x,y) < 0\}$$

and discontinuous demarcation is

$$\Sigma = \{(x,y) \in \mathbb{R}^+ : H(x,y) = 0\}.$$

Let $\mathbf{F}_iH = \langle \nabla H, \mathbf{F}_i \rangle$, where $\langle \cdot, \cdot \rangle$ is the standard scalar product. Then $\mathbf{F}_i^m H = \left\langle \nabla \left(\mathbf{F}_i^{m-1} H \right), \mathbf{F}_i \right\rangle$. Thus the discontinuous demarcation Σ can be distinguished into three regions: 1) sliding region: $\Sigma_s = \{(x,y) \in \Sigma : \mathbf{F}_1H < 0 \text{ and } \mathbf{F}_2H > 0\}$; 2) crossing region: $\Sigma_c = \{(x,y) \in \Sigma : \mathbf{F}_1H \cdot \mathbf{F}_2H > 0\}$; 3) escaping region: $\Sigma_e = \{(x,y) \in \Sigma : \mathbf{F}_1H > 0 \text{ and } \mathbf{F}_2H < 0\}$.

The dynamics of system (2.5) along Σ_s is determined by

$$\begin{pmatrix} \frac{\mathrm{d}x}{\mathrm{d}t} \\ \frac{\mathrm{d}y}{\mathrm{d}t} \end{pmatrix} = \mathbf{F}_s(x,y)(x,y) \in \Sigma_s$$

where $\mathbf{F}_s = \lambda\mathbf{F}_1 + (1-\lambda)\mathbf{F}_2$ with $\lambda = \frac{\mathbf{F}_2 H}{\mathbf{F}_2 H - \mathbf{F}_1 H} \in (0.1)$.

Definition 1 ([24]). *For system* (2.5)*, E^* is a real equilibrium if $\exists i \in \{1,2\}$ so that $\mathbf{F}_i(E^*) = 0$, $E^* \in S_i$; E^* is a virtual equilibrium if $\exists i, j \in \{1,2\}, i \neq j$, so that $\mathbf{F}_i(E^*) = 0$, $E^* \in S_j$; and E^* is a pseudo-equilibrium if $\mathbf{F}_s(E^*) = \lambda\mathbf{F}_1(E^*) + (1-\lambda)\mathbf{F}_2(E^*) = 0, H(E^*) = 0$, and $\lambda = \frac{\mathbf{F}_2 H}{\mathbf{F}_2 H - \mathbf{F}_1 H} \in (0,1)$.*

2.3. Impulsive semi-continuous system

For the given planar model

$$\begin{cases} \dfrac{\mathrm{d}x}{\mathrm{d}t} = \chi_1(x,y), \dfrac{\mathrm{d}y}{\mathrm{d}t} = \chi_2(x,y) & \omega(x,y) \neq 0, \\ \Delta x = I_1(x,y), \Delta y = I_2(x,y) & \omega(x,y) = 0, \end{cases} \tag{2.6}$$

we have:

Definition 2 (Order-k periodic solution [50, 51]). *The solution $\tilde{\mathbf{z}}(t) = (\tilde{x}(t), \tilde{y}(t))$ is called periodic if there exists $n(\geqslant 1)$ satisfying $\tilde{\mathbf{z}}_n = \tilde{\mathbf{z}}_0$. Furthermore, $\tilde{\mathbf{z}}$ is an order-k T-periodic solution with $k \triangleq \min\{j | 1 \leq j \leq n, \tilde{\mathbf{z}}_j = \tilde{\mathbf{z}}_0\}$.*

Lemma 1 (Stability criterion [50, 51]). *The order-k T-periodic solution $\mathbf{z}(t) = (\xi(t), \eta(t))^T$ is orbitally asymptotically stable if $|\mu_q| < 1$, where*

$$\mu_k = \prod_{j=1}^{k} \Delta_j \exp\left(\int_0^T \left[\frac{\partial \chi_1}{\partial x} + \frac{\partial \chi_2}{\partial y} \right]_{(\xi(t),\eta(t))} dt \right),$$

with

$$\Delta_j = \frac{\chi_1^+ \left(\dfrac{\partial I_2}{\partial y}\dfrac{\partial \omega}{\partial x} - \dfrac{\partial I_2}{\partial x}\dfrac{\partial \omega}{\partial y} + \dfrac{\partial \omega}{\partial x} \right) + \chi_2^+ \left(\dfrac{\partial I_1}{\partial x}\dfrac{\partial \omega}{\partial y} - \dfrac{\partial I_1}{\partial y}\dfrac{\partial \omega}{\partial x} + \dfrac{\partial \omega}{\partial y} \right)}{\chi_1 \dfrac{\partial \omega}{\partial x} + \chi_2 \dfrac{\partial \omega}{\partial y}},$$

$\chi_1^+ = \chi_1(\xi(\theta_j^+), \eta(\theta_j^+))$, $\chi_2^+ = \chi_2(\xi(\theta_j^+), \eta(\theta_j^+))$, and χ_1, χ_2, $\frac{\partial I_1}{\partial x}$, $\frac{\partial I_1}{\partial y}$, $\frac{\partial I_2}{\partial x}$, $\frac{\partial I_2}{\partial y}$, $\frac{\partial \omega}{\partial x}$, $\frac{\partial \omega}{\partial y}$ are calculated at $(\xi(\theta_j), \eta(\theta_j))$.

3. Dynamic properties of the Filippov Model (2.1)

For convenience, denote

$$f_1(x,y) \triangleq r(\ln K - \ln x) - \frac{bxy}{(1+hx)(x+g)},$$
$$f_2(x) \triangleq \frac{ebx^2}{(1+hx)(x+g)} - d, \chi_1(x,y) = x f_1(x,y), \chi_2(x,y) = y f_2(x).$$

Since

$$x(t) = x(0)\exp\left(\int_0^t f_1(x,y)\mathrm{d}s \right) \geq 0, y(t) = y(0)\exp\left(\int_0^t f_2(x)\mathrm{d}s \right) \geq 0,$$

then all solutions $(x(t), y(t))$ of Model (2.1) with $x(0) > 0$ and $y(0) > 0$ are positive in the region $\mathbb{D} = \{(x(t), y(t)) | 0 < x \leq K, y \geq 0\}$.

Theorem 1. *For Model* (2.1)*, the solutions are ultimately bounded and uniform in the region* $\mathbb{D}_1$.

Proof. Define $\iota(x(t), y(t)) \triangleq x(t) + y(t)$. Then

$$\frac{\mathrm{d}\iota}{\mathrm{d}t} = \frac{\mathrm{d}x}{\mathrm{d}t} + \frac{\mathrm{d}y}{\mathrm{d}t} = rx(\ln K - \ln x) - \frac{(1-e)bx^2y}{(1+hx)(x+g)} - dy.$$

Take $0 < \theta \leq \min\{r, d\}$, and there is

$$\frac{\mathrm{d}\iota}{\mathrm{d}t} + \theta\iota \leq rx(\ln K - \ln x) + \theta x \triangleq \sigma(x).$$

Obviously, $\sigma'(x) = r(\ln K - r\ln x - 1) - \theta$. If $0 < x < K\mathrm{e}^{\frac{\theta}{r}-1}$, then $\sigma'(x) > 0$. If $x > K\mathrm{e}^{\frac{\theta}{r}-1}$, then $\sigma'(x) < 0$. Then $\sigma(x)$ has a maximum σ^*. Thus $\frac{\mathrm{d}}{\mathrm{d}t}(\iota - \frac{\sigma^*}{\theta}) \leq -\theta(\iota - \frac{\sigma^*}{\theta})$, and then

$$0 \leq \iota\left(x(t), y(t)\right) \leq \left(1 - \mathrm{e}^{-\theta t}\right)\frac{\sigma^*}{\theta} + \iota\left(x(0), y(0)\right)\mathrm{e}^{-\theta t}.$$

For $t \to \infty$, there is $0 \leq \iota\left(x(t), y(t)\right) \leq \frac{\sigma^*}{\theta}$. Therefore, the solutions of Model (2.1) are uniformly bounded in the region

$$\mathbb{D}_1 = \left\{(x, y) \in \mathbb{D} : x(t) + y(t) \leq \frac{\sigma^*}{\theta}\right\} \subset \mathbb{D}.$$

For Model (2.1), the boundary equilibrium $E_K(K, 0)$ always exists. Define

$$\bar{b}(d; p_1) = d(K\mathrm{e}^{-\frac{p_1}{r}} + g)(1 + hK\mathrm{e}^{-\frac{p_1}{r}})/(eK^2\mathrm{e}^{-\frac{2p_1}{r}}),$$
$$\Delta(d) = d^2(1+gh)^2 + 4dg(eb - dh), U(x) = (x+g)(1+hx) + (g - hx^2)(\ln K - \ln x).$$

Theorem 2. *For Model* (2.1)*, if* $b < \bar{b}(d; 0)$*, then* $E_B(K, 0)$ *is locally asymptotically stable. If* $b > \bar{b}(d; 0)$*, there exists a coexistence equilibrium, denoted as* $E_1^* = \left(x_1^*, y_1^*\right)$*, which is locally asymptotically stable if* $U(x_1^*) > 0$*, where*

$$x_1^* = \frac{d(1+gh) + \sqrt{\Delta(d)}}{2(eb - dh)}, y_1^* = r(\ln K - \ln x_1^*)\frac{(x_1^* + g)(1 + hx_1^*)}{bx_1^*}.$$

Proof. For Model (2.1), we have

$$J = \begin{pmatrix} r(\ln K - \ln x) - r - \dfrac{bxy(x + hgx + 2g)}{[(x+g)(1+hx)]^2} & -\dfrac{bx^2}{(x+g)(1+hx)} \\ \dfrac{ebxy(x + hgx + 2g)}{[(x+g)(1+hx)]^2} & \dfrac{ebx^2}{(x+g)(1+hx)} - d \end{pmatrix}.$$

1) For $E_K(K, 0)$, we have

$$J|_{(K,0)} = \begin{pmatrix} -r & -\frac{bK^2}{(K+g)(1+hK)} \\ 0 & \frac{ebK^2}{(K+g)(1+hK)} - d \end{pmatrix}.$$

Then $\lambda_1 = -r < 0$ and $\lambda_2 = \frac{ebK^2}{(K+g)(1+hx)} - d$. Therefore, $E_B(K, 0)$ is locally asymptotically stable if $b < b(d; 0)$.

2) Since

$$f_{1_x} = -\frac{r}{x} - \frac{by(g - hx^2)}{[(x+g)(1+hx)]^2}, f_{1_y} = -\frac{bx}{(x+g)(1+hx)}, f_{2_x} = \frac{ebx(x + hgx + 2g)}{[(x+g)(1+hx)]^2},$$

then for E_1^*, we have

$$\lambda_1\lambda_2 = -x_1^* y_1^* f_{1_y} f_{2_x} > 0, \lambda_1 + \lambda_2 = x_1^* f_{1_x}.$$

If $U(x_1^*) > 0$ holds, then $\lambda_1\lambda_2 > 0, \lambda_1 + \lambda_2 < 0$, i.e., E_1^* is locally asymptotically stable.

3.1. Complex dynamics of Model (2.2)

Let

$$\mathbf{F_1}(x,y) = \left(rx(\ln K - \ln x) - \frac{bx^2y}{(1+hx)(x+g)}, \frac{ebx^2y}{(1+hx)(x+g)} - dy\right)^T,$$
$$\mathbf{F_2}(x,y) = \left(rx(\ln K - \ln x) - \frac{bx^2y}{(1+hx)(x+g)} - p_1x, \frac{ebx^2y}{(1+hx)(x+g)} - dy + (q_1 - q_2)y\right)^T,$$
$$\mathbf{F_3}(x,y) = \left(rx(\ln K - \ln x) - \frac{bx^2y}{(1+hx)(x+g)} - p_1x, \frac{ebx^2y}{(1+hx)(x+g)} - dy - q_2y\right)^T.$$

Then systems (2.2) and (2.3) can be described as

$$\begin{pmatrix} \frac{\mathrm{d}x}{\mathrm{d}t} \\ \frac{\mathrm{d}y}{\mathrm{d}t} \end{pmatrix} = \mathbf{F_i}(x,y), (x,y) \in G_i, i = 1,2,3, \tag{3.1}$$

where

$$G_1 = \left\{(x,y) \in \mathbb{R}_+^2 : x < x_{ET}\right\},$$
$$G_2 = \left\{(x,y) \in \mathbb{R}_+^2 : x > x_{ET}, y < y_{ET}\right\}, G_3 = \left\{(x,y) \in \mathbb{R}_+^2 : x > x_{ET}, y > y_{ET}\right\}.$$

The switching boundaries are, respectively,

$$\Sigma_1 = \left\{(x,y) \in \mathbb{R}_+^2 : x = x_{ET}, y < y_{ET}\right\},$$
$$\Sigma_2 = \left\{(x,y) \in \mathbb{R}_+^2 : x = x_{ET}, y > y_{ET}\right\}, \Sigma_3 = \left\{(x,y) \in \mathbb{R}_+^2 : x > x_{ET}, y = y_{ET}\right\}.$$

Let $\mathbf{n_1} = (1,0)$ and $\mathbf{n_2} = (0,1)$ be the normal vector for Σ_1 and Σ_3. If $\exists\Sigma_{ij} \subset \Sigma_i$ such that the trajectory of $\mathbf{F_i}(x,y)$ approaches or moves away from Σ_i ($i \in \{1,2,3\}$) on both sides, then a sliding domain exists, and the dynamics on Σ_i can be determined by means of the Filippov convex method.

3.1.1. Dynamic behavior of the sub-models

The dynamic behavior of the model in G_1 can be referred to Section 3.2. The model in G_2 is described as follows:

$$\begin{cases} \frac{\mathrm{d}x}{\mathrm{d}t} = rx(\ln K - \ln x) - \frac{bx^2y}{(1+hx)(x+g)} - p_1x, \\ \frac{\mathrm{d}y}{\mathrm{d}t} = \frac{ebx^2y}{(1+hx)(x+g)} - dy + (q_1 - q_2)y. \end{cases} \tag{3.2}$$

Theorem 3. *Model* (3.2) *always has an equilibrium* $E_{\overline{B}}(Ke^{-\frac{p_1}{r}}, 0)$. *If* $q_1 < q_2 + d$ *and* $b < b(d - q_1 + q_2; p_1)$, *then* $E_{\overline{B}}(Ke^{-\frac{p_1}{r}}, 0)$ *is locally asymptotically stable. If* $q_1 < q_2 + d$ *and* $b > \bar{b}(d + q_2 - q_1, p_1)$, *Model* (3.2) *has a coexistence equilibrium, denoted as* $E_2^* = \left(x_2^*, y_2^*\right)$, *which is locally asymptotically stable if* $U(x_2^*) > 0$, *where*

$$x_2^* = \frac{(d - q_1 + q_2)(1 + gh) + \sqrt{\Delta(d - q_1 + q_2)}}{2[eb + h(q_1 - q_2 - d)]}, y_2^* = [r(\ln K - \ln x_2^*) - p_1]\frac{(x_2^* + g)(1 + hx_2^*)}{bx_2^*}.$$

Similarly, the model in G_3 is described as follows:

$$\begin{cases} \dfrac{\mathrm{d}x}{\mathrm{d}t} = rx(\ln K - \ln x) - \dfrac{bx^2y}{(1 + hx)(x + g)} - p_1x, \\ \dfrac{\mathrm{d}y}{\mathrm{d}t} = \dfrac{ebx^2y}{(1 + hx)(x + g)} - dy - q_2y. \end{cases} \tag{3.3}$$

Theorem 4. *Model* (3.3) *always has an equilibrium* $E_{\overline{B}}(Ke^{-\frac{p_1}{r}}, 0)$. *If* $b < b(d + q_2; p_1)$, *then* $E_{\overline{B}}$ *is locally asymptotically stable. If* $b > b(d + q_2; p_1)$, *Model* (3.3) *has a coexistence equilibrium, denoted as* $E_3^* = (x_3^*, y_3^*)$, *which is locally asymptotically stable if* $U(x_3^*) > 0$, *where*

$$x_3^* = \frac{(d + q_2)(1 + gh) + \sqrt{\Delta(d - q_1 + q_2)}}{2[eb - h(d + q_2)]}, y_3^* = [r(\ln K - \ln x_3^*) - p_1]\frac{(x_3^* + g)(1 + hx_3^*)}{bx_3^*}.$$

3.1.2. Dynamic behavior of Model (2.2)

It is assumed that

(H1) $p_1 < r$;

(H2) $\dfrac{d(1 + gh) + \sqrt{\Delta(d)}}{2(eb - dh)} < K$;

(H3) $q_1 - q_2 - d < 0, \dfrac{(d - q_1 + q_2)(1 + gh) + \sqrt{\Delta(d - q_1 + q_2)}}{2[eb + h(q_1 - q_2 - d)]} < K\mathrm{e}^{-\frac{p_1}{r}}$;

(H4) $\dfrac{(d + q_2)(1 + gh) + \sqrt{\Delta(d + q_2)}}{2[eb - h(d + q_2)]} < K\mathrm{e}^{-\frac{p_1}{r}}$.

For Model (2.2), we have $x_1^* < x_2^* < x_3^*$ when $q_1 < q_2$ and $x_2^* < x_1^* < x_3^*$ when $q_2 < q_1 < q_2 + d$.

Define

$$y_{ET1} = [r(\ln K - \ln x_{ET}) - p_1]\frac{(x_{ET} + g)(1 + hx_{ET})}{bx_{ET}},$$
$$y_{ET2} = r(\ln K - \ln x_{ET})\frac{(x_{ET} + g)(1 + hx_{ET})}{bx_{ET}},$$

where $y_{ET2} > 0$ and $y_{ET1} < y_{ET2}$.

First, we will discuss the sliding mode domain on Σ_1 and the corresponding dynamics. Since

$$\begin{aligned} < \mathbf{F_1}, \mathbf{n_1} >|_{(x,y)\in\Sigma_1} &= x_{ET}\left[r(\ln K - \ln x_{ET}) - \frac{bx_{ET}y}{(1 + hx_{ET})(x_{ET} + g)}\right], \\ < \mathbf{F_2}, \mathbf{n_1} >|_{(x,y)\in\Sigma_1} &= x_{ET}\left[r(\ln K - \ln x_{ET}) - \frac{bx_{ET}y}{(1 + hx_{ET})(x_{ET} + g)} - p_1\right], \end{aligned} \tag{3.4}$$

then the sliding mode domain on Σ_1 does not exist if $y_{ET} < y_{ET1}$. When $y_{ET} > y_{ET1}$, we have

$$\Sigma_{11} = \{(x, y) \in \Sigma_1 | \max\{0, y_{ET1}\} < y < \min\{y_{ET2}, y_{ET}\}\}. \tag{3.5}$$

Next, the Filippov convex method is used, i.e.,

$$\frac{\mathrm{d}X}{\mathrm{d}t} = \lambda \mathbf{F_1} + (1 - \lambda)\mathbf{F_2}, (x, y) \in \Sigma_{11}, \tag{3.6}$$

where

$$\lambda = \frac{< \mathbf{F_2}, \mathbf{n_1} >}{< \mathbf{F_2}, \mathbf{n_1} > - < \mathbf{F_1}, \mathbf{n_1} >},$$

and the sliding mode dynamics of Eq (3.1) along Σ_{11} is determined by the following system:

$$\begin{cases} \dfrac{\mathrm{d}x}{\mathrm{d}t} = 0, \\ \dfrac{\mathrm{d}y}{\mathrm{d}t} = \left[\dfrac{ebx_{ET}{}^2}{(1 + hx_{ET})(x_{ET} + g)} - d\right] y + \dfrac{q_1 - q_2}{p_1}\left[r(\ln K - \ln x_{ET}) - \dfrac{bx_{ET}y}{(1 + hx_{ET})(x_{ET} + g)}\right] y. \end{cases} \tag{3.7}$$

Let $\varsigma_1 = ebx_{ET}{}^2 + (1 + hx_{ET})(x_{ET} + g)\left[\frac{r(q_1-q_2)}{p_1}(\ln K - \ln x_{ET}) - d\right]$. Then a positive equilibrium $E_{a1}(x_{ET}, y_{a1})$ exists, where $y_{a1} = \dfrac{p_1\varsigma_1}{bx_{ET}(q_1 - q_2)} > 0$. Therefore

$$y_{a1} - y_{ET2} = \frac{p_1}{bx_{ET}(q_1 - q_2)}[ebx_{ET}{}^2 - d(1 + hx_{ET})(x_{ET} + g)].$$

If $x_1^* < x_{ET}$, then $y_{a1} > y_{ET2}$, i.e., E_{a1} is not located in Σ_{11}, and then E_{a1} is not a pseudo-equilibrium. If $x_1^* > x_{ET}$, then $y_{a1} < y_{ET2}$.

Similarly, we have

$$y_{a1} - y_{ET1} = \frac{p_1}{bx_{ET}(q_1 - q_2)}[ebx_{ET}{}^2 + (q_1 - q_2 - d)(1 + hx_{ET})(x_{ET} + g)].$$

If $x_2^* > x_{ET}$, then $y_{a1} < y_{ET1}$, i.e., E_{a1} is not located in Σ_{11}, and then E_{a1} is not a pseudo-equilibrium. If $x_2^* < x_{ET}$, then $y_{a1} > y_{ET1}$. Therefore, $y_{ET1} < y_{a1} < y_{ET2}$. When $y_{a1} < y_{ET}$, E_{a1} is the pseudo-equilibrium.

Second, we will discuss the sliding mode domain on Σ_2 and the dynamic characteristics on the sliding mode. Since

$$\begin{aligned} < \mathbf{F_1}, \mathbf{n_1} >|_{(x,y)\in\Sigma_2} &= x_{ET}\left[r(\ln K - \ln x_{ET}) - \frac{bx_{ET}y}{(1 + hx_{ET})(x_{ET} + g)}\right], \\ < \mathbf{F_3}, \mathbf{n_1} >|_{(x,y)\in\Sigma_2} &= x_{ET}\left[r(\ln K - \ln x_{ET}) - \frac{bx_{ET}y}{(1 + hx_{ET})(x_{ET} + g)} - p_1\right], \end{aligned} \tag{3.8}$$

then the sliding mode domain on Σ_2 does not exist if $y_{ET} > y_{ET2}$; When $y_{ET} < y_{ET2}$, we have

$$\Sigma_{22} = \{(x, y) \in \Sigma_2 | \max\{y_{ET1}, y_{ET}\} < y < y_{ET2}\}. \tag{3.9}$$

Therefore, when $y_{ET} > y_{ET2}$, there is no sliding mode domain on Σ_2. When $y_{ET} < y_{ET2}$, the sliding mode domain of the system (3.1) on Σ_2 can be expressed as Eq (3.9).

According to the Filippov convex method, we have

$$\frac{\mathrm{d}X}{\mathrm{d}t} = \lambda F_1 + (1-\lambda)F_3, (x,y) \in \Sigma_{22}, \tag{3.10}$$

where

$$\lambda = \frac{< \mathbf{F_3}, \mathbf{n_1} >}{< \mathbf{F_3}, \mathbf{n_1} > - < \mathbf{F_1}, \mathbf{n_1} >},$$

and the sliding mode dynamics of equation (3.1) along Σ_{22} is determined by the following system:

$$\begin{cases} \dfrac{\mathrm{d}x}{\mathrm{d}t} = 0, \\ \dfrac{\mathrm{d}y}{\mathrm{d}t} = \left[\dfrac{ebx_{ET}{}^2}{(1+hx_{ET})(x_{ET}+g)} - d\right]y - \dfrac{q_2}{p_1}\left[r(\ln K - \ln x_{ET}) - \dfrac{bx_{ET}y}{(1+hx_{ET})(x_{ET}+g)}\right]y. \end{cases} \tag{3.11}$$

Let $\varsigma_2 = (1+hx_{ET})(x_{ET}+g)\left[\frac{rq_2}{p_1}(\ln K - \ln x_{ET}) + d\right] - ebx_{ET}{}^2$. Then the system (3.11) has a positive equilibrium $E_{a2}(x_{ET}, y_{a2})$, where $y_{a2} = \frac{p_1\varsigma_2}{q_2 b x_{ET}} > 0$. Obviously,

$$y_{a2} - y_{ET2} = -\frac{p_1}{q_2 b x_{ET}}[ebx_{ET}{}^2 - d(1+hx_{ET})(x_{ET}+g)].$$

If $x_1^* > x_{ET}$, then $y_{a2} > y_{ET2}$, i.e., E_{a2} is not located in Σ_{22}. If $x_1^* < x_{ET}$, then $y_{a2} < y_{ET2}$. Similarly, we have

$$y_{a2} - y_{ET1} = -\frac{p_1}{q_2 b x_{ET}}[ebx_{ET}{}^2 - (d+q_2)(1+hx_{ET})(x_{ET}+g)].$$

If $x_3^* < x_{ET}$, then $y_{a2} < y_{ET1}$, i.e, E_{a2} is not located in Σ_{22}. If $x_3^* > x_{ET}$, then $y_{a2} > y_{ET1}$. Therefore $y_{ET1} < y_{a2} < y_{ET2}$. If $y_{ET1} < y_{ET} < y_{a2}$ or $y_{ET} < y_{ET1}$, then E_{a2} is located in Σ_{22} and is a pseudo-equilibrium.

Finally, we will discuss the sliding mode domain on Σ_3 and the dynamic characteristics of the sliding mode. We have

$$\begin{aligned} < \mathbf{F_2}, \mathbf{n_2} >|_{(x,y)\in\Sigma_3} &= y_{ET}\left[\frac{ebx^2}{(1+hx)(x+g)} - d + q_1 - q_2\right], \\ < \mathbf{F_3}, \mathbf{n_2} >|_{(x,y)\in\Sigma_3} &= y_{ET}\left[\frac{ebx^2}{(1+hx)(x+g)} - d - q_2\right]. \end{aligned} \tag{3.12}$$

According to Eq (3.12), $< \mathbf{F_2}, \mathbf{n_2} >|_{(x,y)\in\Sigma_3} > < \mathbf{F_3}, \mathbf{n_2} >|_{(x,y)\in\Sigma_3}$. If $x_3^* < x_{ET}$, then the system (3.1) does not have a sliding mode domain on Σ_3. If $x_2^* < x_{ET} < x_3^*$, it is found through Eq (3.12) that the system (3.1) can be expressed in the sliding mode domain on Σ_3 as

$$\Sigma_{33} = \{(x,y) \in \Sigma_3 | \, x_{ET} < x < x_3^*\}. \tag{3.13}$$

According to the Filippov convex method, we have

$$\frac{\mathrm{d}X}{\mathrm{d}t} = \lambda F_2 + (1-\lambda)F_3, (x,y) \in \Sigma_{33}, \tag{3.14}$$

where

$$\lambda = \frac{< \mathbf{F_3}, \mathbf{n_2} >}{< \mathbf{F_3}, \mathbf{n_2} > - < \mathbf{F_2}, \mathbf{n_2} >}.$$

The sliding mode dynamics of Eq (3.1) along Σ_{11} is determined by the following system:

$$\begin{cases} \dfrac{\mathrm{d}x}{\mathrm{d}t} = rx(\ln K - \ln x) - \dfrac{bx^2 y_{ET}}{(1+hx)(x+g)} - p_1 x, \\ \dfrac{\mathrm{d}y}{\mathrm{d}t} = 0. \end{cases} \tag{3.15}$$

Then

$$[r(\ln K - \ln x) - p_1](1+hx)(x+g) - bxy_{ET} = 0. \tag{3.16}$$

If the root $x = x_b > 0$ of Eq (3.16) satisfies Eq (3.13), then $E_b(x_b, y_{ET})$ of the system (3.15) is a pseudo-equilibrium, and if it does not satisfy Eq (3.13), then E_b is not a pseudo-equilibrium.

4. Dynamic analysis of the impulse pest-management model

For Model (2.4), let

$$y = \widehat{y}(x) \triangleq \frac{r(\ln(K) - \ln(x))(1+hx)(x+g)}{bx}.$$

The curve $y = \widehat{y}(x)$ intersects with $x = x_{ET}$ and $x = (1-p_1)x_{ET}$ at $P(x_{ET}, y_P)$ ($y_P = \widehat{y}(x_{ET})$) and $R_0((1-p_1)x_{ET}, y_{R_0})$. The trajectory passing through P is denoted by γ_1, and it goes backward and intersects $y = \widehat{y}(x)$ at $H(x_H, y_H)(y_H = \widehat{y}(x_H))$. If $x_H < (1-p_1)x_{ET}$, then denote $Q_1((1-p_1)x_{ET}, y_{Q_1})$, $Q_2((1-p_1)x_{ET}, y_{Q_2})$ as the intersection points between γ_1 and $x = (1-p_1)x_{ET}$ with $y_{Q_1} < y_{Q_2}$. The trajectory passing through R_0 is denoted by γ_2. If $\gamma_2 \cap \{x = x_{ET}\} \neq \varnothing$, then denote $R_1(x_{ET}, y_{R_1})$ as the intersection point between γ_2 and $x = x_{ET}$. The curve γ_2 defines a function $y = y(x, y_{R_0})$ on the interval $[(1-p_1)x_{ET}, x_{ET}]$ with

$$\frac{\mathrm{d}y}{\mathrm{d}x} = \frac{\frac{ebx^2 y}{(1+hx)(x+g)} - dy}{rx(\ln K - \ln x) - \frac{bx^2 y}{(1+hx)(x+g)}} \triangleq \varphi(x, y), y((1-p_1)x_{ET}, y_{R_0}) = y_{R_0},$$

which takes the form

$$y = y(x, y_{R_0}) = y_{R_0} + \int_{(1-p_1)x_{ET}}^{x} \varphi(u, y(u, y_{R_0}))\mathrm{d}u.$$

4.1. Accurate domains of $\mathcal{M}$ and $\mathcal{N}$

For Model (2.4), we have $\mathcal{M} = \{(x, y) \mid x = x_{ET}, y > 0\}$. The trajectory of the system (2.4) with $x_0 < x_{ET}$ can reach $\mathcal{M}_1 = \{(x, y) | x = x_{ET}, 0 \le y \le y_P\} \subset \mathcal{M}$, which is called the effective impulse set, denoted by $\mathcal{M}_{eff}$. The corresponding effective phase set is denoted by $\mathcal{N}_{eff}$. Moreover, define $\mathcal{M}_2 = \{(x, y) \mid x = x_{ET}, 0 \le y \le y_{R_1}\} \subset \mathcal{M}_1$.

Since $\Delta y = -q_2 y + \frac{\tau}{1+ly}$, then define

$$\rho(y) \triangleq (1-q_2)y + \frac{\tau}{1+ly}.$$

Obviously, the function $\rho(y)$ reaches a minimum at $y = \widehat{y}$, where $\widehat{y} \triangleq \frac{\sqrt{\tau l(1-q_2)} - (1-q_2)}{l(1-q_2)}$. Denote $R(x_{ET}, \widehat{y}) \in \mathcal{M}$, and its phase point is $R^+\left((1-p_1)x_{ET}, \rho(\widehat{y})\right)$.

Define

$$x_{ET}^1 \triangleq \max\{x_{ET} | y(x_{ET}, R_0)\}, \quad x_{ET}^2 \triangleq \max\{x_{ET} | y(x_{ET}, Q_1) \geq y_{Q_2}/2\}.$$

Denote

$$\tau_1 \triangleq \frac{1-q_2}{l}, \quad \tau_2 \triangleq \frac{(1-q_2)(1+ly_P)^2}{l}, \quad \tau_3 \triangleq \frac{(1-q_2)(1+ly_{R_1})^2}{l}.$$

The exact domains of $\mathcal{M}$ and $\mathcal{N}$ can be determined by $\text{SIGN}(\rho'(y))$ and $\text{SIGN}(\widehat{y})$, which will be discussed in the following two situations:

Case I: $x_{ET}^1 < x_{ET} \leq x_{ET}^2$.

For this situation, $\mathcal{M}_{eff} = \mathcal{M}_1$. To determine $\mathcal{N}_{eff}$, we are required to judge the magnitude between $\widehat{y}$ and y_P. Denote $\Lambda = [0, y_{Q_1}] \bigcup [y_{Q_2}, +\infty)$.

i) $\tau \geq \tau_1$, then $\widehat{y} \leq 0$. For $\forall y \in [0, y_P]$, $\rho' \geq 0$ holds, and then $\tau \leq \rho(y) \leq \rho(y_P)$ for $y \in [0, y_P]$. Denote $\Lambda_{11} = [\tau, \rho(y_P)]$, $\Lambda_1 = \Lambda \bigcap \Lambda_{11}$, and $\mathcal{N}_{eff} = \mathcal{N}_1 = \{(x^+, y^+) | \, x^+ = (1-p_1)x_{ET}, y^+ \in \Lambda_1\}$.

ii) $\tau_1 < \tau < \tau_2$, then $0 < \widehat{y} < y_P$. For $\forall y \in [0, \widehat{y}]$, $\rho' \leq 0$ holds, and then $\rho(\widehat{y}) \leq \rho(y) \leq \tau$ for $y \in [0, \widehat{y}]$. Denote $\Lambda_{21} = [\rho(\widehat{y}), \tau]$, $\Lambda_{21}^* = \Lambda \bigcap \Lambda_{21}$, and $\mathcal{N}_{21} = \left\{(x^+, y^+) | \, x^+ = (1-p_1)x_{ET}, y^+ \in \Lambda_{21}^*\right\}$. Similarly, for $\forall y \in (\widehat{y}, y_P]$, $\rho' > 0$ holds, i.e., $\rho(\widehat{y}) < \rho(y) \leq \rho(y_P)$. Denote $\Lambda_{22} = (\rho(\widehat{y}), \rho(y_P)]$, $\Lambda_{22}^* = \Lambda \bigcap \Lambda_{22}$, and $\mathcal{N}_{22} = \left\{(x^+, y^+) | \, x^+ = (1-p_1)x_{ET}, y^+ \in \Lambda_{22}^*\right\}$. Thus, we have $\mathcal{N}_{eff} = \mathcal{N}_2 = \mathcal{N}_{21} \bigcup \mathcal{N}_{22}$.

iii) $\tau \leq \tau_2$, then $\widehat{y} \geq y_P$. For $\forall y \in [0, y_P]$, $\rho' \leq 0$ holds, i.e., $\rho(y_P) \leq \rho(y) \leq \tau$. Denote $\Lambda_{33} = [\rho(y_P), \tau]$ and $\Lambda_3 = \Lambda \bigcap \Lambda_{33}$. Then $\mathcal{N}_{eff} = \mathcal{N}_3 = \{(x^+, y^+) | \, x^+ = (1-p_1)x_{ET}, y^+ \in \Lambda_3\}$.

Case II: $x_{ET} \geq x_{ET}^1$.

For this situation, $\mathcal{M}_{eff} = \mathcal{M}_2$. Similar to the discussion in case I, we have

i) $\tau \geq \tau_1$. Then $\mathcal{N}_{eff} = \mathcal{N}_4 = \{(x^+, y^+) | \, x^+ = (1-p_1)x_{ET}, y^+ \in \Lambda_4\}$, where $\Lambda_4 = [\tau, \rho(y_{R_1})]$.

ii) $\tau_1 < \tau < \tau_3$. For $\forall y \in [0, \widehat{y}]$, we have $\mathcal{N}_{51} = \{(x^+, y^+) | \, x^+ = (1-p_1)x_{ET}, y^+ \in \Lambda_{21}\}$. Similarly, for $\forall y \in (\widehat{y}, y_{R_1}]$, denote $\Lambda_{52} = (\rho(\widehat{y}), \rho(y_{R_1})]$, and then $\mathcal{N}_{52} = \{(x^+, y^+) | x^+ = (1-p_1)x_{ET}, y^+ \in \Lambda_{52}\}$. Therefore, $\mathcal{N}_{eff} = \mathcal{N}_5 = \mathcal{N}_{51} \bigcup \mathcal{N}_{52}$.

iii) $\tau \leq \tau_3$. Then $\mathcal{N}_{eff} = \mathcal{N}_6 = \{(x^+, y^+) | \, x^+ = (1-p_1)x_{ET}, y^+ \in \Lambda_6\}$ with $\Lambda_6 = [\rho(y_{R_1}), \tau]$.

4.2. Poincaré map

Denote $G_i(x_{ET}, y_i) \in \mathcal{M}$, $G_i^+((1-p_1)x_{ET}, y_i^+) \in \mathcal{N}$, $i = 0, 1, 2, ...$, where $G_i^+ = \mathbf{I}(G_i)$. Since G_i^+ and G_{i+1} lie on the same trajectory $\gamma_{G_i^+}$, then we have $y_{i+1} = \varpi(y_i^+)$ and $y_{i+1}^+ = \psi(y_i^+)$, where

$$\psi(y_i^+) \triangleq (1-q_2)\varpi(y_i^+) + \frac{\tau}{1 + l\varpi(y_i^+)}.$$

If $\exists \hat{y} \in \mathcal{N}$ such that $\psi(\hat{y}) = \hat{y}$, then Model (2.4) admits an order-1 periodic trajectory. Next, we will investigate the monotonicity of $\psi(y)$ with $\tau > 0$ for situations I and II.

Case I: $x_{ET}^1 < x_{ET} \leq x_{ET}^2$.

i) $\tau \geq \tau_1$. $\rho(y)$ monotonically increases on $[0, y_P]$, and then the map $\psi(y)$ monotonically increases on $[0, y_{Q_1}]$ and monotonically decreases on $[y_{Q_2}, +\infty)$.

ii) $\tau_1 < \tau < \tau_2$. we have $\rho'(y) < 0$ for $y \in [0, \widehat{y}]$ and $\rho'(y) > 0$ for $y \in (\widehat{y}, y_P]$. Denote $y_{S_1} = \min\{y : \psi(y) = y_{R^+}\}$, $y_{S_2} = \max\{y : \psi(y) = y_{R^+}\}$. Then $\psi(y)$ monotonically increases on $[y_{S_1}, y_{Q_1}]$, $[y_{S_2}, +\infty)$ and monotonically decreases on the interval $[0, y_{S_1}]$, $[y_{Q_2}, y_{S_2}]$, respectively.

iii) $\tau \le \tau_2$. $\rho(y)$ monotonically decreases on $[0, y_P]$, and then the map $\psi(y)$ monotonically decreases on $[0, y_{Q_1}]$ and monotonically increases on $[y_{Q_2}, +\infty)$.

Case II: $x_{ET} \ge x_{ET}^1$.

i) $\tau \ge \tau_1$. Then $\psi'(y) > 0$ for $y \in [0, y_{R_0}]$ and $\psi'(y) < 0$ for $y \in [y_{R_0}, +\infty)$.

ii) $\tau_1 < \tau < \tau_3$. Denote $y_{V_1} = \min\{y : \psi(y) = y_{R^+}\}$ and $y_{V_2} = \max\{y : \psi(y) = y_{R^+}\}$. Then $\psi(y)$ monotonically decreases on $[0, y_{V_1}]$ and $[y_{R_0}, y_{V_2}]$, and monotonically increases on $[y_{V_1}, y_{R_0}]$ and $[y_{V_2}, +\infty)$.

iii) $\tau \le \tau_3$. The map $\psi(y)$ monotonically decreases on $[0, y_{R_0}]$ and monotonically increases on $[y_{R_0}, +\infty)$.

4.3. Order-1 periodic trajectory

4.3.1. Natural enemy extinction periodic trajectory

For Model (2.4) with $\tau = 0$, if $y_0 \equiv 0$, then $y \equiv 0$ holds. Thus Model (2.4) is degenerated to

$$\begin{cases} \dfrac{\mathrm{d}x}{\mathrm{d}t} = rx(\ln K - \ln x), x < x_{ET}, \\ \Delta x = -p_1 x(t), x = x_{ET}. \end{cases} \tag{4.1}$$

Let $x = \widetilde{x}(t)$ be the solution of equation

$$\frac{\mathrm{d}x}{\mathrm{d}t} = rx(\ln K - \ln x)$$

with initial value $\widetilde{x}(0) = x_0 \triangleq (1 - p_1)x_{ET}$. Define

$$T_0 \triangleq \frac{1}{r}\left(\ln\ln\frac{K}{(1-p_1)x_{ET}} - \ln\ln\frac{K}{x_{ET}}\right).$$

We have $\tilde{x}(T_0) = x_{ET}$ and $\tilde{x}(T_0^+) = x_0$. Thus, $\mathbf{z}(t) = (\widetilde{x}(t), 0)$ $((k-1)T_0 < t \le kT_0, k \in N_+)$ is a natural enemy extinction periodic trajectory.

Theorem 5. *The natural enemy extinction period trajectory $\mathbf{z}(t) = (\widetilde{x}(t), 0)$ $((k-1)T_0 < t \le kT_0$, $k \in N_+)$ is orbitally asymptotically stable if $q_2 > \hat{q}$, where*

$$\hat{q} \triangleq 1 - \tau l - \frac{(\ln K - \ln x_{ET}) \exp\left(-\int_0^{T_0}\left(r(\ln K - \ln\tilde{x}) - r + \frac{eb\tilde{x}^2}{(\tilde{x}+g)(1+h\tilde{x})} - d\right)dt\right)}{(1-p_1)(\ln K - \ln(1-p_1)x_{ET})}.$$

Proof. For Model (4.1), we have

$$I_1(x, y) = -p_1 x, I_2(x, y) = -q_2 y + \frac{\tau}{1 + ly}, \omega(x, y) = x - x_{ET}.$$

Then

$$\frac{\partial \chi_1}{\partial x} = r(\ln K - \ln x) - r - \frac{bxy(x + hgx + 2g)}{[(x+g)(1+hx)]^2}, \frac{\partial \chi_2}{\partial y} = \frac{ebx^2}{(x+g)(1+hx)} - d,$$
$$\frac{\partial I_1}{\partial x} = -p_1, \frac{\partial I_1}{\partial y} = 0, \frac{\partial I_2}{\partial x} = 0, \frac{\partial I_2}{\partial y} = -q_2 - \frac{l\tau}{(1+ly)^2}, \frac{\partial \omega}{\partial x} = 1, \frac{\partial \omega}{\partial y} = 0.$$

Through calculation, we have

$$\tilde{\kappa} = \frac{(1 - q_2 - l\tau)(1 - p_1)(\ln K - \ln(1 - p_1)x_{ET})}{\ln K - \ln x_{ET}}$$

and

$$\int_{0^+}^{T} \left(\frac{\partial \chi_1}{\partial x} + \frac{\partial \chi_2}{\partial y} \right)_{(\widetilde{x},0)} \mathrm{d}t = \int_0^{T_0} \left(r(\ln K - \ln \tilde{x}) - r + \frac{eb\tilde{x}^2}{(\tilde{x}+g)(1+h\tilde{x})} - d \right) \mathrm{d}t.$$

Thus,

$$\hat{\rho} = \widetilde{\kappa} \exp\left(\int_0^{T_0} \left(r(\ln K - \ln \tilde{x}) - r + \frac{eb\tilde{x}^2}{(\tilde{x}+g)(1+h\tilde{x})} - d \right) \mathrm{d}t \right).$$

Therefore, if $q_2 > \hat{q}$, we have $\hat{\rho} < 1$, and by Lemma 1, $\mathbf{z}(t) = (\widetilde{x}(t), 0)$ $((k-1)T_0 < t \le kT_0, k \in N_+)$ is orbitally asymptotically stable.

4.3.2. Coexisting order-1 periodic trajectory

Denote that the points P, R_1 are mapped to the points $P^+\left((1-p_1)x_{ET}, (1-q_2)y_P + \frac{\tau}{1+ly_P}\right)$ and $R_1^+\left((1-p_1)x_{ET}, (1-q_2)y_{R_1} + \frac{\tau}{1+ly_{R_1}}\right)$, respectively, after a single impulse. Denote $W((1-p_1)x_{ET}, \tau)$.

Case I: $x_{ET}^1 < x_{ET} \le x_{ET}^2$.

Define

$$q_2^* \triangleq 1 - \frac{y_{Q_2}}{2y_P}, l^* \triangleq \frac{\sqrt{1 + 4y_P(1-q_2)/(y_{Q_1} - (1-q_2)y_P)} - 1}{2y_P},$$
$$\tilde{\tau}_1 \triangleq (1+ly_P)(y_{Q_1} - (1-q_2)y_P), \tilde{\tau}_2 \triangleq (1+ly_P)(y_{Q_2} - (1-q_2)y_P),$$
$$\hat{\tau}_1 = (1-q_2)\frac{[1 + ly_{Q_2}/(1-q_2)]^2}{4l}, \hat{\tau}_2 = (1-q_2)\frac{[1 + ly_{Q_1}/(1-q_2)]^2}{4l}, \tau_4 \triangleq (1-q_2)\frac{1+ly_P}{l}.$$

Obviously, $\tau_4 < \tau_2$ and for $q_2 \le q_2^*$, we have $l > \max\{l^*, 0\}$.

1) For $\tau = \tilde{\tau}_2$, we have $\psi(y_{Q_2}) = y_{P^+} = y_{Q_2}$.

2) For $\tau > \tilde{\tau}_2$, we have $\psi(y_{Q_2}) = y_{P^+} > y_{Q_2}$. Then

- 2-a) for $\tau \ge \tau_2$, $W$is the highest after the pulse, while P^+ is the lowest after the pulse. Then $\psi(\tau) < \tau$, $\psi(y_{P^+}) > y_{P^+}$, and thus $\exists y' \in (y_{P^+}, \tau)$ such that $\psi(y') = y'$.
- 2-b) for $\tilde{\tau}_2 < \tau < \tau_2$, if $\tau \ge \hat{\tau}_2$, then $\rho(\widehat{y}) \ge y_{Q_2}$. Since the point R^+ is the lowest point after the pulse, then $\psi(y_{R^+}) > y_{R^+}$. If $\tau > \tau_4$, we have $\tau > y_{P^+}$. Then W is the highest point after the impulse, i.e., $\psi(\tau) < \tau$. If $\tau \le \tau_4$, we have $\tau \le y_{P^+}$. Then P^+ is the highest point after the impulse, i.e., $\psi(y_{P^+}) < y_{P^+}$. Combine the above two aspects and it can be concluded that $\exists y'' \in (y_{R^+}, \max\{\tau, y_{P^+}\})$ such that $\psi(y'') = y''$. While for $\tau < \hat{\tau}_2$, we have $\rho(\widehat{y}) < y_{Q_2}$. In such a case, ψ is not defined on $[\rho(\widehat{y}), y_{Q_2})$ and it is uncertain whether a fixed point of ψ exists or not.

3) When $\tilde{\tau}_1 < \tau < \tilde{\tau}_2$, then $y_{Q_1} < y_{P^+} < y_{Q_2}$. If $\tau \geq \hat{\tau}_1$, then $\rho(\widehat{y}) \geq y_{Q_1}$, i.e., ψ does not have a fixed point. While for $\tau < \hat{\tau}_1$, we have $\rho(\widehat{y}) < y_{Q_1}$. In such a case, it is uncertain whether a fixed point of ψ exists or not.

4) When $0 < \tau < \tilde{\tau}_1$, and then $\psi(y_{Q_1}) = y_{P^+} < y_{Q_1}$. If $\tau > \tau_1$, the point R^+ is the lowest point after the pulse, then $\psi(y_{R^+}) > y_{R^+}$, i.e., $\psi(y)$ has a fixed point on (y_{R^+}, y_{Q_1}). If $\tau \leq \tau_1$, the point W is the lowest point after the pulse, and then $\psi(\tau) > \tau$, i.e., $\psi(y)$ has a fixed point on (τ, y_{Q_1}).

Case II: $x_{ET} \geq x_{ET}^1$.

Define $\tilde{\tau} \triangleq (1 + ly_{R_1})(y_{R_0} - (1 - q_2)y_{R_1})$.

1) For $\tau = \tilde{\tau}$, we have $\psi(y_{R_0}) = y_{R_1^+} = y_{R_0}$.

2) For $\tau > \tilde{\tau}$, we have $\psi(y_{R_0}) = y_{R_1^+} > y_{R_0}$. Then

- 2-a) for $\tau \geq \tau_3$, since R_1^+ and W are the lowest and highest points after the pulse, then we have $\psi(y_{R_1^+}) > y_{R_1^+}$, $\psi(\tau) < \tau$, and thus $\exists y' \in (y_{R_1^+}, \tau)$ such that $\psi(y') = y'$;
- 2-b) for $\tilde{\tau} < \tau < \tau_3$ and if $\tau > y_{R_1^+}$, then $\psi(\tau) < \tau$; if $\tau \leq y_{R_1^+}$, then $\psi(y_{R_1^+}) > y_{R_1^+}$. On the other hand, take the point A in a small neighborhood near the point R_0, i.e., $A \in \bigcup(R_0, \delta)$. A is above R_0. By the continuity of the impulse function and the Poincaré map, we have $\psi(y_A) > y_A$. Therefore, the map $\psi(y)$ has a fixed point on $(y_A, \max\{y_{R_1^+}, \tau\})$.

3) When $\tau < \tilde{\tau}$, then $\psi(y_{R_0}) = y_{R_1^+} < y_{R_0}$. If $\tau > \tau_1$, we have $\psi(y_{R^+}) > y_{R^+}$. If $\tau \leq \tau_1$, we have $\psi(\tau) > \tau$. Combine the above two aspects and it can be concluded that $\exists y'' \in (\max\{y_{R^+}, \tau\}, y_{R_0})$ such that $\psi(y'') = y''$.

To sum up, we have:

Theorem 6. *For the situation of $x_{ET} \geq x_{ET}^1$, Model* (2.4) *admits an order-1 periodic trajectory. While for the situation of $x_{ET}^1 < x_{ET} \leq x_{ET}^2$, Model* (2.4) *admits an order-1 periodic trajectory if $\tau < \tilde{\tau}_1$ or $\tau \geq \max\{\tilde{\tau}_2, \hat{\tau}_2\}$.*

Let $\widetilde{\mathbf{z}}(t) = (\xi(t), \eta(t))$ $((k-1)T < t \leq kT, k \in N_+)$ be the T-periodic trajectory of the system (2.4) with initial values $A_0((1 - p_1)x_{ET}, y_{A_0})$. The trajectory intersects $\mathcal{M}$ at $A_0^-(\xi(T), \eta(T))$, where $\xi(T) = x_{ET}, \eta(T) = y_0$, and then it is pulsed to $\mathcal{N}$ at $A_0^+(\xi(T^+), \eta(T^+))$. Thus, $\xi(T^+) = (1 - p_1)x_{ET}, \eta_1(T^+) = (1 - q_2)y_0 + \frac{\tau}{1+ly_0} = y_{A_0}$.

Theorem 7. *The T-periodic trajectory $\widetilde{\mathbf{z}}(t) = (\xi(t), \eta(t))$ $((k-1)T < t \leq kT, k \in N_+)$ with initial values $\left((1 - p_1)x_{ET}, (1 - q_2)y_0 + \frac{\tau}{1+ly_0}\right)$ is orbitally asymptotically stable if*

$$\int_0^T \left(r(\ln K - \ln x) - r - \frac{bxy(x + hgx + 2g)}{[(x + g)(1 + hx)]^2} + \frac{ebx^2}{(x + g)(1 + hx)} - d \right)_{(\xi(t),\eta(t))} dt < \ln(\hat{\kappa}),$$

where

$$\hat{\kappa} = \frac{r(\ln K - \ln x_{ET}) - \frac{bx_{ET}y_0}{(x_{ET}+g)(1+hx_{ET})}}{(1 - p_1)\left(1 - q_2 - \frac{l\tau}{(1+ly_0)^2}\right)\left[r(\ln K - \ln(1 - p_1)x_{ET}) - \frac{b(1-p_1)x_{ET}\left((1-q_2)y_0 + \frac{\tau}{1+ly_0}\right)}{((1-p_1)x_{ET}+g)(1+h(1-p_1)x_{ET})}\right]}.$$

Proof. The proof can be referred to that in Theorem 5 and is, therefore omitted.

5. Computer simulations

For the purpose of simulation, it is assumed that $r = 1.5$, $K = 120$, $b = 0.595$, $h = 0.92$, $e = 0.8$, $d = 0.5$ and $g = 0.8$.

5.1. *Verification of Model* (2.1)

When $b = 0.595$, the interior equilibrium $E_1^* = (54.7, 103.1)$ is locally asymptotically stable, as presented in Figure 1. When b increases to 0.61, a limit cycle occurs, as presented in Figure 2. The effect of the maximum search rate on pests and natural enemies in the coexistence steady state is presented in Figure 3, and it is obvious that x_1^* decreases with increasing b, while y_1^* increases and then decreases with increasing b. Therefore, increasing the search rate for pests helps to reduce the number of pests.

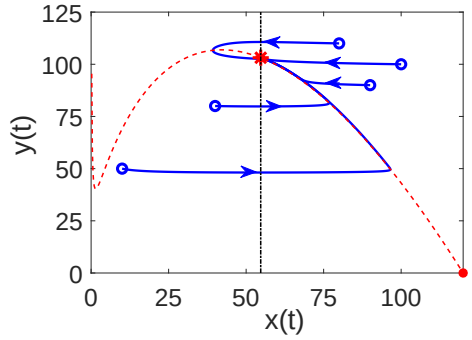

Figure 1. Tendencies of Model (2.1) in case of $b = 0.595$.

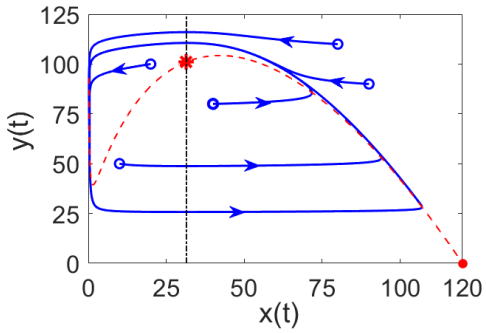

Figure 2. Tendencies of Model (2.1) in case of $b = 0.61$.

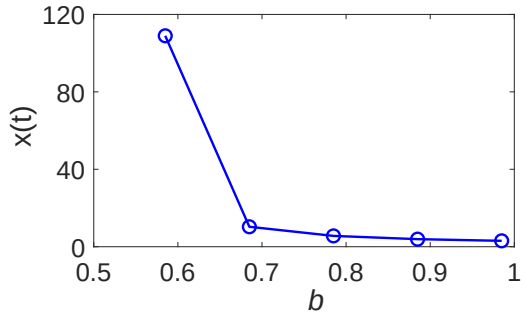

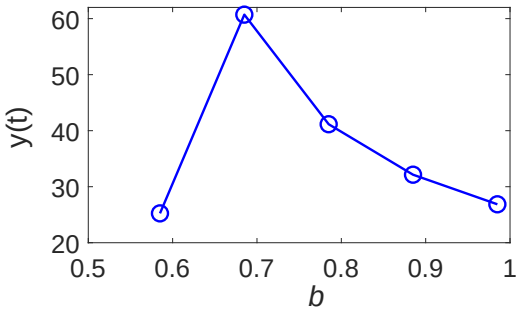

Figure 3. Relationship between the number of pests (natural enemies) and the maximum search rate at the steady state.

5.2. *Verification of Model* (2.2)

When $p_1 = 0.25$, $q_1 = 0.5$ and $q_2 = 0.007$, the positive equilibrium of the G_1 region is $E_1^* = (54.707, 103.1337)$, the positive equilibrium of the G_2 region is $E_2^* = (0.1229, 141.532)$, and the positive equilibrium of the G_3 region is $E_3^* = (92.5247, 20.443)$. When $x_{ET} = 100$ and $y_{ET} = 110$,

there is $x_2^* < x_3^* < x_{ET}$, $x_1^* < x_{ET}$, $y_{ET1} = 3.6997$ and $y_{ET2} = 43.0879$. The sliding mode domain of Model (3.1) on Σ_1 can be represented as $\Sigma_{11} = \{(x, y) \in \Sigma_1 | 3.6997 < y < 43.0879\}$, and there is no pseudo-equilibrium on Σ_1, as illustrated in Figure 4(a). When $x_{ET} = 80$ and $y_{ET} = 110$, there is $x_2^* < x_{ET} < x_3^*$, $x_1^* < x_{ET}$, $y_{ET1} = 45.3593$ and $y_{ET2} = 77.0172$. The sliding mode domain of Model (3.1) on Σ_1 can be represented as $\Sigma_{11} = \{(x, y) \in \Sigma_1 | 45.3593 < y < 77.0172\}$, and there is no pseudo-equilibrium on Σ_1, as presented in Figure 4(b).

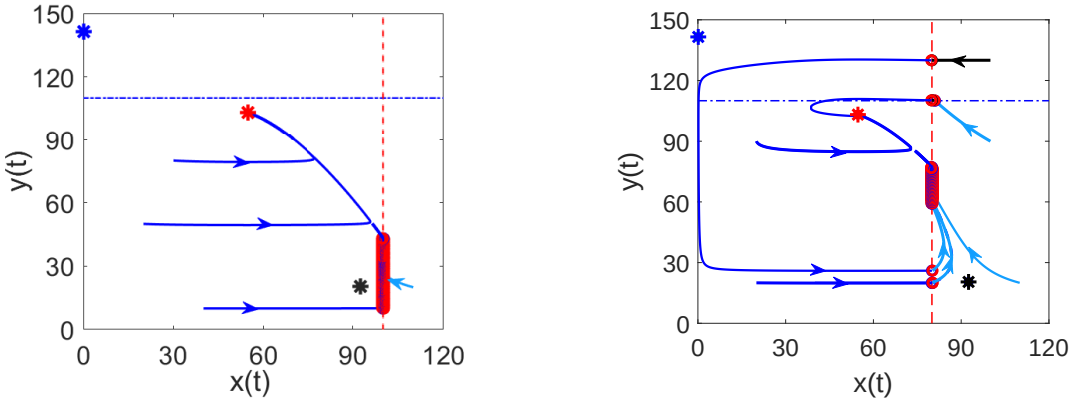

Figure 4. The dynamic behavior of Model (2.2) for $y_{ET} = 110$ and different pest control levels: (a) $x_{ET} = 100$; (b) $x_{ET} = 80$.

5.3. *Verification of Model* (2.4)

When $q_2 = 0.11$, for $x_{ET} = 62.667$, the periodic trajectory of Model (2.4) is presented by changing the killing rate p_1 of the prey, the amount of predator released τ, and the value of the parameter l. When $\tau = 0$, $p_1 = 0.5$ and $l = 0.02$, the natural enemy extinction periodic trajectory is orbitally asymptotically stable (Figure 5(a)). To prevent the extinction of natural enemies, we are required to release natural enemies in an appropriate amount. When $\tau = 5$, the natural enemy extinction periodic trajectory loses its stability and an order-1 periodic trajectory occurs (Figure 5(b)).

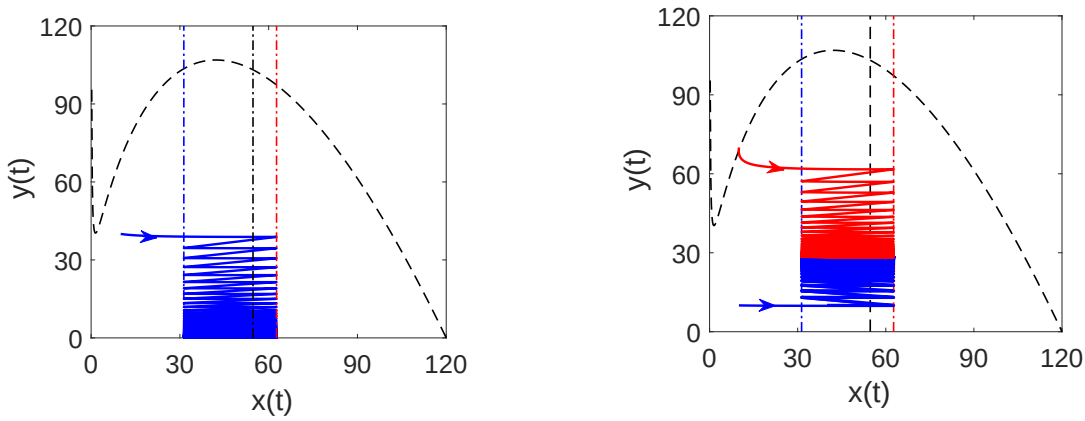

Figure 5. Illustration of the trajectory of Model (2.4) for $l = 0.02$ and different τ: (a) $\tau = 0$, (b) $\tau = 5$.

Next, the accurate domains of $\mathcal{M}$ and $\mathcal{N}$ for different cases are presented as well as the order-1 periodic trajectory (Figure 6). The accurate domains of $\mathcal{M}$ and $\mathcal{N}$ are marked in red and blue solid lines, respectively. When $p_1 = 0.5$, H lies on the left side of the phase set. The schematic diagram of the exact domain of the phase set and pulse set, and the order-1 periodic trajectories for different cases are presented in subfigures Figure 6(a)–(c). When $p_1 = 0.6$, H lies on the right side of the phase set. The schematic diagram of the accurate domain of $\mathcal{M}$ and $\mathcal{N}$ and the order-1 periodic trajectories for different cases are presented in subfigures Figure 6(d)–(f).

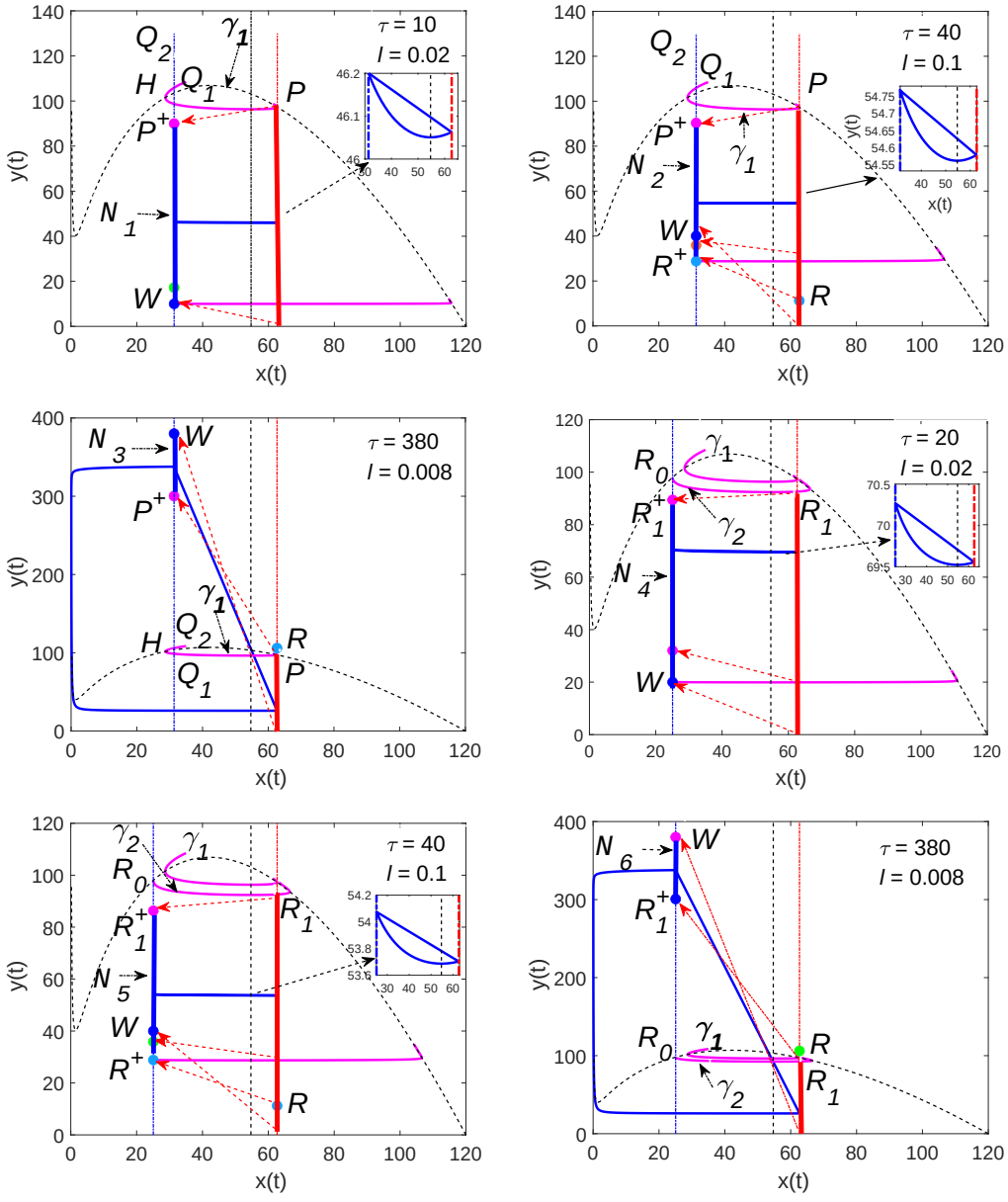

Figure 6. Presentation of the order-1 periodic trajectory of Model (2.4).

When $p_1 = 0.5$, $l = 0.02$, $\tau = 10$, $b = 0.595$ and $x_{ET} = 50$, E^* is locally asymptotically stable, and Model (2.4) admits an order-1 periodic trajectory for $x_{ET} < x_{ET}^1$, as presented in Figure 7.

Finally, order-n periodic solutions are presented for different τ and l. When $b = 0.595$, E^* is locally

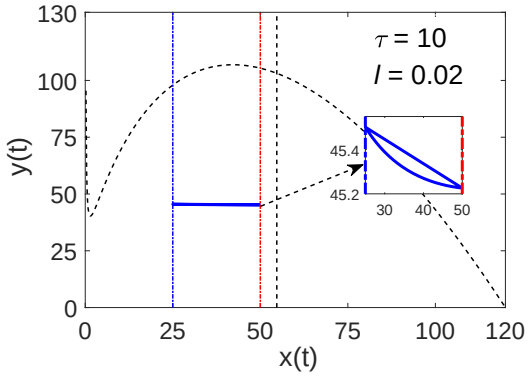

Figure 7. Presentation of the order-1 periodic trajectory of Model (2.4) for $x_{ET} < x_{ET}^1$.

asymptotically stable. For control parameters $l = 0.03$, $\tau = 120$, $x_{ET} = 62.667$ or $l = 0.002$, $\tau = 40$, $x_{ET} = 62.667$, Model (2.2) admits an order-k periodic trajectory, as presented in subfigures 8(a) and (b). When $b = 0.61$, Model (2.1) admits a limit cycle. For $x_{ET} = 50$, Model (2.2) admits an order-k periodic trajectory, as presented in subfigures 8(c)–8(f).

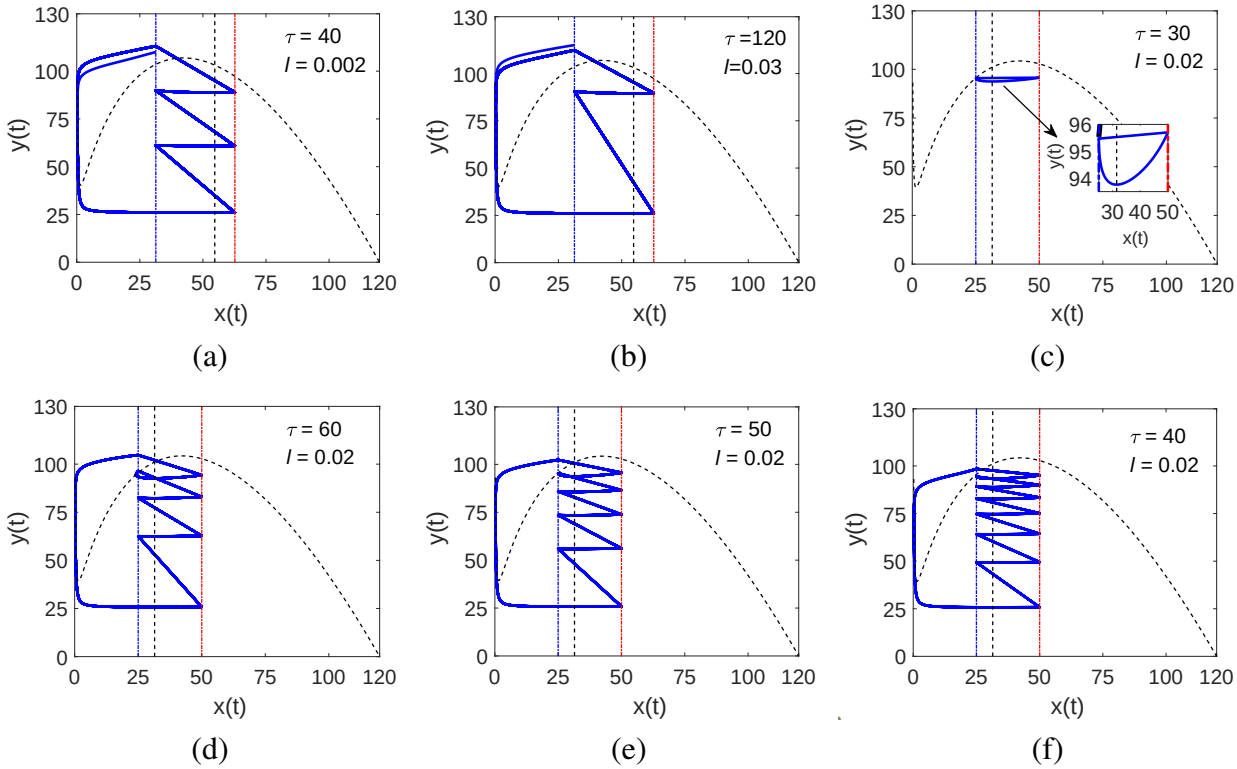

Figure 8. Presentation of the order-k periodic trajectory of Model (2.4) for different situations.

6. Conclusions and discussion

Pests are important factors that harm agricultural production. In order to effectively control the spread of pests, a pest-natural enemy model with a variable search rate and threshold dependent feedback control was proposed. The dynamic properties such as the existence, positivity, and boundedness of solutions for continuous systems were discussed, and the results show that pests and natural enemies will not increase indefinitely due to system constraints (Theorem 1). In addition, it is shown that the natural enemy's searching rate b plays an important role in determining the dynamics of the system, i.e., when b is smaller than the level $\bar{b}(d;0)$, the predators in the system will go to extinction and when b is greater than $\bar{b}(d;0)$, there exists a steady state E^* at which the natural enemies and the pests in the system keep a balance. Moreover, the steady state is locally asymptotically stable as long as $U(x^*) > 0$ (Theorems 2–4, Figure 1). When $U(x^*) < 0$, the stability is lost and a limit cycle surrounding E^* is obtained (Figure 2). The relationship between the number of pests (natural enemies) and the maximum search rate at the steady state was presented in Figure 3.

To prevent the spread of pests, two different types of control strategies were adopted. The first is a non-smooth control and the model is described by a Filippov system with two warning thresholds. By analyzing the sliding dynamics, we discussed the existence of pseudo-equilibrium E_p (Figure 4). The pseudo-equilibrium E_p is a new state of the control system at which the pests and the natural enemies keep a balance and the pest populations can be controlled at appropriate levels, which in turn indicates the effectiveness of the control. The second is an intermittent control with an economic threshold. When the pests reach the economic threshold, manual intervention is carried out by spraying pesticides and releasing a certain amount of natural enemies. For the control model, the accurate domain of the phase set was presented and the Poincaré map was constructed, through which the conditions for the existence of the order-1 periodic trajectories were presented (Theorems 5 and 6 and Figures 5–7). The order-1 periodic solution provides a possibility for periodic pest control, thus avoiding the need and difficulty of implementing pest population monitoring. The stability of the order-1 periodic trajectory was also verified (Theorems 5 and 7). This ensures the robustness of the control, and even if there is a condition monitoring error, it can still converge to the periodic solution of the system, thus providing a guarantee for the periodic control. We also presented the order-k periodic solutions in numerical simulations (Figure 8), which further explain the complexity of the control system and the necessity of maintaining the stability of the system. The results illustrate the complex dynamics of the proposed models, which can serve as a valuable reference for the advancement of sustainable agricultural practices and the control of pests.

Use of AI tools declaration

The authors declare they have not used Artificial Intelligence (AI) tools in the creation of this article.

Acknowledgement

The work was supported by the National Natural Science Foundation of China (No. 11401068).

Conflict of interest

The authors declare that there is no known competing financial interests to influence the work in this paper.

References

1. W. C. Liu, X. M. Zhu, F. Y. Zhuo, Strengthening the implementation of prevention and control responsibilities along the main line of implementing the "Regulations on the Prevention and Control of Crop Diseases and Pests" to ensure national food security, *China Plant Protect.*, **41** (2021), 5–9.
2. M. X. Chen, H. M. Srivastava, Existence and stability of bifurcating solution of a chemotaxis model, *Proc. Am. Math. Soc.*, **151** (2023), 4735–4749. https://doi.org/10.1090/proc/16536
3. Q. Zhang, S. Tang, X. Zou, Rich dynamics of a predator-prey system with state-dependent impulsive controls switching between two means, *J. Differ. Equations*, **364** (2023), 336–377. https://doi.org/10.1016/j.jde.2023.03.030
4. Y. Tian, X. R. Yan, K. B. Sun, Dual effects of additional food supply and threshold control on the dynamics of a Leslie-Gower model with pest herd behavior, *Chaos Solitons Fractals*, **185** (2024), 115163. https://doi.org/10.1016/j.chaos.2024.115163
5. X. R. Yan, Y. Tian, K. B. Sun, Dynamic analysis of a delayed pest-natural enemy model: Triple effects of non-monotonic functional response, additional food supply and habitat complexity, *Int. J. Biomath.*, (2024), 2450062. https://doi.org/10.1142/S1793524524500621
6. M. X. Chen, R. C. Wu, Dynamics of a harvested predator-prey model with predator-taxis, *Bull. Malays. Math. Sci. Soc.*, **46** (2023), 76. https://doi.org/10.1007/s40840-023-01470-w
7. H. Nie, S. X. Xin, H. Y. Shu, Effects of diffusion and advection on predator-prey dynamics in closed environments, *J. Differ. Equations*, **367** (2023), 290–331. https://doi.org/10.1016/j.jde.2023.05.004
8. H. K. Qi, B. Liu, Stationary distribution of a stochastic reaction-diffusion predator-prey model with additional food and fear effect, *Appl. Math. Lett.* **150** (2024), 108978. https://doi.org/10.1016/j.aml.2023.108978
9. M. X. Chen, S. Ham, Y. Choi, H. Kim, J. Kim, Pattern dynamics of a harvested predator-prey model, *Chaos Solitons Fractals*, **176** (2023),114153. https://doi.org/10.1016/j.chaos.2023.114153
10. Y. H. Sun, Invasion analysis of a reaction-diffusion-advection predator-prey model in spatially heterogeneous environment, *Nonlinear Anal. Real World Appl.*, **77** (2024), 104048. https://doi.org/10.1016/j.nonrwa.2023.104048
11. M. X. Chen, Pattern dynamics of a Lotka-Volterra model with taxis mechanism, *Appl. Math. Comput.*, **484** (2025), 129017. https://doi.org/10.1016/j.amc.2024.129017
12. A. J. Lotka, Eelements of physical biology, *Am. J. Public Health*, **21** (1926), 341–343. https://doi.org/10.2307/2298330
13. V. Volterra, Fluctuations in the abundance of a species considered mathematically, *Nature*, **118** (1926), 558–560. https://doi.org/10.1038/119012b0

14. B. Gompertz, On the nature of the function expressive of the law of human mortality, and on a new mode of determining the value of life contingencies, *Philos. Trans. R. Soc. London*, **115** (1825), 513–583. https://www.jstor.org/stable/107756
15. G. F. Gause, N. P. Smaragdova, A. A. Witt, Further studies of interaction between predators and prey, *J. Anim. Ecol.*, **5** (1936), 1–18. https://doi.org/10.2307/1087
16. F. E. Smith, Population dynamics in daphnia magna and a new model for population growth, *Ecology*, **44** (1963), 651–663. https://doi.org/10.2307/1933011
17. C. S. Holling, The functional response of predators to prey density and its role in mimicry and population regulation, *Mem. Entomol. Soc. Can. Suppl.*, **45** (1965), 5–60. https://doi.org10.4039/entm9745fv
18. M. Hassell, C. Varley, New inductive population model for insect parasites and its bearing on biological control, *Nature*, **223** (1969), 1133–1177. https://doi.org 10.1038/2231133a0.
19. R. E. Kooij, A. Zegeling, A predator-prey model with Ivlev's functional response, *J. Math. Anal. Appl.*, **198** (1996), 473–489. https://doi.org/10.1006/jmaa.1996.0093
20. Y. Kuang, E. Beretta, Global qualitative analysis of a ratio-dependent predator-prey system, *J. Math. Biol.*, **36** (1998), 389–406. https://doi.org/10.1007/s002850050105
21. P. M. Stoner, Fitting the exponential function and the Gompertz function by the method of least squares, *J. Am. Stat. Assoc.*, **35** (1941), 515–518. https://www.jstor.org/stable/2278959
22. K. Y. Liu, X. Z. Meng, L. S. Chen, A new stage structured predator-prey Gomportz model with time delay and impulsive perturbations on the prey, *Appl. Math. Comput.*, **196** (2008), 705–719. https://doi.org/10.1016/j.amc.2007.07.020
23. K. M. C. Tjørve, E Tjørve, The use of Gompertz models in growth analyses, and new Gompertz-model approach: An addition to the Unified-Richards family, *PLoS One*, **12** (2017), e0178691. https://doi.org/10.1371/journal.pone.0178691
24. M. P. Hassell, H. N. Comins, Sigmoid functional responses and population stability, *Theor. Popul. Biol.*, **14** (1978), 62–67. https://doi.org/10.1016/0040-5809(78)90004-7
25. H. Guo, Y. Tian, K. B. Sun, X.Y. Song, Dynamic analysis of two fishery capture models with a variable search rate and fuzzy biological parameters, *Math. Biosci. Eng.*, **20** (2023), 21049–21074. https://doi.org/10.3934/mbe.2023931
26. A. Wang, Y. Xiao, R. Smith, Using non-smooth models to determine thresholds for microbial pest management, *J. Math. Biol.*, **78** (2019), 1389–1424. https://doi.org/10.1007/s00285-018-1313-z
27. W. J. Li, J. C. Ji, L. H. Huang, J. F. Wang, Bifurcations and dynamics of a plant disease system under non-smooth control strategy, *Nonlinear Dyn.*, **99** (2020), 3351–3371. https://doi.org/10.1007/s11071-020-05464-2
28. W. X. Li, L. H. Huang, J. F. Wang, Global asymptotical stability and sliding bifurcation analysis of a general Filippov-type predator-prey model with a refuge, *Appl. Math. Comput.*, **405** (2021), 126263. https://doi.org/10.1016/j.amc.2021.126263
29. N. S. Chong, B. Dionne, R. Smith, An avian-only Filippov model incorporating culling of both susceptible and infected birds in combating avian influenza, *J. Math. Biol.*, **73** (2016), 751–784. https://doi.org/10.1007/s00285-016-0971-y

30. X. Jiao, X. Li, Y. Yang, Dynamics and bifurcations of a Filippov Leslie-Gower predator-prey model with group defense and time delay, *Chaos Solitons Fractals*, **162** (2022), 112436. https://doi.org/10.1016/j.chaos.2022.112436

31. C. C. García, Bifurcations on a discontinuous Leslie-Grower model with harvesting and alternative food for predators and Holling II functional response, *Commun. Nonlinear Sci. Numer. Simul.*, **116** (2023), 106800. https://doi.org/10.1016/j.cnsns.2022.106800

32. W. X. Li, L. H. Huang, J. F. Wang, Global dynamics of Filippov-type plant disease models with an interaction ratio threshold, *Math. Method Appl. Sci.*, **43** (2020), 6995–7008. https://doi.org/10.1002/mma.6450

33. W. X. Li, Y. M. Chen, L. H. Huang, J. F. Wang, Global dynamics of a filippov predator-prey model with two thresholds for integrated pest management, *Chaos Solitons Fractals*, **157** (2022), 111881. https://doi.org/10.1016/j.chaos.2022.111881

34. B. Liu, Y. Zhang, L. Chen, The dynamical behaviors of a Lotka-Volterra predator-prey model concerning integrated pest management, *Nonlinear Anal. Real World Appl.*, **6** (2005), 227–243. https://doi.org/10.1016/j.nonrwa.2004.08.001

35. X. Y. Song, Y. F. Li, Dynamic behaviors of the periodic predator-prey model with modified Leslie-Gower Holling-type II schemes and impulsive effect, *Nonlinear Anal. Real World Appl.*, **9** (2008), 64–79. https://doi.org/10.1016/j.nonrwa.2006.09.004

36. X. R. Yan, Y. Tian, K. B. Sun, Effects of additional food availability and pulse control on the dynamics of a Holling-(p+1) type pest-natural enemy model, *Electron. Res. Arch.*, **31** (2023). 6454–6480. https://doi.org/10.3934/era.2023327

37. J. Jia, Z. Zhao, J. Yang, A. Zeb, Parameter estimation and global sensitivity analysis of a bacterial-plasmid model with impulsive drug treatment, *Chaos Solitons Fractals*, **183** (2024), 114901. https://doi.org/10.1016/j.chaos.2024.114901

38. S. Y. Tang, R. A. Cheke, State-dependent impulsive models of integrated pest management (IPM) strategies and their dynamic consequences, *J. Math. Biol.*, **50** (2005), 257–292. https://doi.org/10.1007/s00285-004-0290-6

39. S. Y. Tang, W. Pang, R. A. Cheke, J. H. Wu, Global dynamics of a state-dependent feedback control system, *Adv. Differ. Equations*, **2015** (2015), 1–70. https://doi.org/10.1186/s13662-015-0661-x

40. Y. Tian, H. Li, K. B. Sun, Complex dynamics of a fishery model: Impact of the triple effects of fear, cooperative hunting and intermittent harvesting, *Math. Comput. Simul.*, **218** (2024), 31–48. https://doi.org/10.1016/j.matcom.2023.11.024

41. L. Nie, Z. Teng, H. Lin, J. Peng, Qualitative analysis of a modified Leslie-Gower and Holling-type II predator-prey model with state dependent impulsive effects, *Nonlinear Anal.-RWA*, **11** (2010), 1364–1373. https://doi.org/10.1016/j.nonrwa.2009.02.026

42. X. R. Yan, Y. Tian, K. B. Sun, Dynamic analysis of additional food provided non-smooth pest-natural enemy models based on nonlinear threshold control, *J. Appl. Math. Comput.*, 2024, in press. https://doi.org/10.1007/s12190-024-02318-7

43. Y. Tian, Y. Liu, K. B. Sun, Complex dynamics of a predator-prey fishery model: The impact of the Allee effect and bilateral intervention, *Electron. Res. Arch.*, **32** (2024), 6379–6404. https://doi.org/10.3934/era.2024297

44. L. Nie, Z. Teng, H. Lin, J. Peng, The dynamics of a Lotka-Volterra predator-prey model with state dependent impulsive harvest for predator, *Biosystems*, **98** (2009), 67–72. https://doi.org/10.1016/j.biosystems.2009.06.001

45. W. Li, J. Ji, L. Huang, Global dynamic behavior of a predator-prey model under ratio-dependent state impulsive control, *Appl. Math. Model.*, **77** (2020), 1842–1859. https://doi.org/10.1016/j.apm.2019.09.033

46. Q. Zhang, S. Tang, Bifurcation analysis of an ecological model with nonlinear state-dependent feedback control by poincaré map defined in phase set, *Commun. Nonlinear Sci. Numer. Simul.*, **108** (2022), 106212. https://doi.org/10.1016/j.cnsns.2021.106212

47. Y. Tian, Y. Gao, K. B. Sun, Global dynamics analysis of instantaneous harvest fishery model guided by weighted escapement strategy, *Chaos Solitons Fractals*, **164** (2022), 112597. https://doi.org/10.1016/j.chaos.2022.112597

48. Y. Tian, Y. Gao, K. B. Sun, Qualitative analysis of exponential power rate fishery model and complex dynamics guided by a discontinuous weighted fishing strategy, *Commun. Nonlinear Sci. Numer. Simul.*, **118** (2023), 107011. https://doi.org/10.1016/j.cnsns.2022.107011

49. Y. Tian, Y. Gao, K. B. Sun, A fishery predator-prey model with anti-predator behavior and complex dynamics induced by weighted fishing strategies, *Math. Biosci. Eng.*, **20** (2023), 1558–1579. https://doi.org/10.3934/mbe.2023071

50. Y. Tian, H. Guo, K. B. Sun, Complex dynamics of two prey-predator harvesting models with prey refuge and interval-valued imprecise parameters, *Math. Method Appl. Sci.*, **46** (2023). 14278–14298. https://doi.org/10.1002/mma.9319

51. H. Guo, Y. Tian, K. Sun, X. Y. Song, Study on dynamic behavior of two fishery harvesting models: effects of variable prey refuge and imprecise biological parameters, *J. Appl. Math. Comput.*, **69** (2023), 4243–4268. https://doi.org/10.1007/s12190-023-01925-0

AIMS Press